CrossMark

Preparation of nanocrystalline Mg doped CdSe thin films and their optical, photoluminescence, electrical and structural characterization

Prashant K. Sahu[1] · Ruby Das[1] · Rajesh Lalwani[1]

Abstract Phosphors used are mostly rare earth doped complex structures. A simple and unique material system of CdSe:Mg nanocrystalline thin films, which efficiently absorb UV (235 nm) and emit broad spectrum of green-yellow region has been prepared by chemical bath deposition method with average particle size of 52.3 nm, measured using AFM images. The optical absorption studies found that CdSe thin film has direct optical band gap, E_g of 2.62 eV that shows a blue shift of 0.88 eV compared to the bulk E_g value. Optical, electrical, structural and morphological properties were studied by UV–Vis–NIR spectrophotometer, photoluminescence (PL) emission spectra, dc two-probe method, X-ray diffraction (XRD), and atomic force microscope (AFM). Measured electrical resistivity decreased with increase of doping concentration. Activation energy was also calculated. The results confirm that the CdSe:Mg thin films are in the pure cubic phase. The magnesium concentrations also affect the nanocrystalline nature of the CdSe thin films. The optical band gap and surface roughness of CdSe thin films mostly decrease with 5% doping of Mg. The effect of Mg doping on refractive index, extinction coefficient and other optical parameters was also investigated.

1 Introduction

Nanocrystalline (nc) thin films are an important category material that can find potential applications in photo electronic devices. Fundamental studies of cadmium selenide (CdSe), a well-known direct band gap II–VI semiconductor, have been reported for its applications in such fields as photodetectors, field-effect transistors (FETs), field emitters, solar cells, light-emitting diodes (LEDs), memory devices, biosensors and biomedical imaging [1–5]. Recently it has been found that size-tunable CdSe QDs have great potential in diagnosis of cancerous cells [6]. Due to strong quantum confinement effects and intrinsic dipole moments, nanocrystals have a large extinction coefficient that leads to rapid charge separation [7]. Inorganic semiconductor nanostructures find size and shape-dependent electrical and optical properties and can be processed with various methods.

Doping is a widely used method to tailor the electrical and optical properties of semiconductors [2]. PL properties of the Doped semiconductor nanoparticles have been studied extensively because of their excellent luminescence properties. Alkaline earth aluminates ($SrAl_2O_4$) doped with rare earth ions show high chemical stability and bright emission in the visible region [8]. The ZnMgO nanophosphor film with 25% Mg exhibited maximum PL output [9]. For tuning the band gap of ZnS nanoparticles, doping of Mg metal was found to be a good technique [10]. Reddy et al. [11] have synthesized Mg-doped ZnS hierarchical spheres using hydrothermal method. They have observed blue–green photoluminescence with tunable intensity and peak position, depending on the Mg content. Two strong peaks situated at the green emission (at 528 nm) and red emission (at 655–695 nm) and two weak UV emission peaks at 378 and 417 nm, respectively were indicated in sixfold symmetrical Mg-doped CdS nanowires fabricated through high

✉ Ruby Das
   dwijendrad@yahoo.co.in

   Prashant K. Sahu
   prashantsahu_27@yahoo.co.in

[1] Department of Applied Physics, Bhilai Institute of Technology, Durg, C.G. 491001, India

temperature vapor–solid deposition process [12]. Cadmium selenide thin films have been deposited on non-conducting glass by CSVS technique [13] and stainless steel substrates [6]. CdSe nanocrystals with a zinc blende structure allowed apparent Mg doping of (~9.8 at%) [14].

Sputtering, spray pyrolysis, electro deposition etc. are variety of methods reported for the preparation of CdSe thin film [1, 15]. Magnesium chalcogenides (MgX, X = O, S, Se, Te) are of technological and scientific interest because they are wide band gap semiconductors. The nanocrystalline MgSe films of direct optical band gap 2.45 eV and thickness 188 ± 20 nm were deposited at 523 K temperature using $MgCl_2$ and SeO_2 precursors MBE and MOVCVD have also been used to deposit MgSe thin films [16]. This material is not well understood due to its hygroscopic nature and unstable zinc blende structure. The Mg based II–VI materials have shown a new way to cover a wide range of wavelengths in optoelectronic devices [17]. The literature survey revealed that no reports are available on preparation of CdSe:Mg nanoparticle thin film by simple chemical method. Since CdSe:Mg has advantage over CdSe in changing the band gap of the material (for MgSe, $E_g = 2.4$ eV, for CdSe, $E_g = 1.7$ eV), this subsequently influences its electro-optical properties. Structure sensitive control of electrical and optical properties in such materials will be useful in many ways [18]. Therefore, appropriate structural characterization of the films is necessary. Crystallinity, crystal phase, lattice constant and grain size of these structures are strongly dependent on the deposition conditions. The present work focuses on the effect of doping alkaline earth metal Mg in CdSe using a simple and low cost chemical route method. To the best of our knowledge, literature on Mg doped CdSe is scarce.

2 Materials and methods

2.1 Preparation of CdSe:Mg thin film

Nanocrystalline cadmium selenide (CdSe) thin films were prepared by chemical bath deposition (CBD) method. Formation of nucleation centers is highly essential for best quality films. Hence clean amorphous glass surface was a necessary requirement. We have chosen substrates of commercial quality microscopic glass slide of dimensions 24 mm × 75 mm. Initially they were dipped in nitric acid for 48 h. After detergent wash, placed them in ultrasonic cleaner with triple distilled water and finally dried at room temperature. This method is based on the controlled release of the ions in a bath containing solution of cadmium acetate, magnesium chloride and freshly prepared and filtered selenium precursor solution, sodium selenosulphate. Though difficult, using reflux condenser along with magnetic stirrer attached

with the hot plate, we successfully prepared sodium selenosulphate, just prior to deposition by dissolving selenium pellets in a sodium sulfite solution at 80 °C with stirring for a period of 5 h. The high purity (99.99%) selenium pellets and chemicals of AR grade (Sigma Aldrich) were used here. To prepare 0.4M CdSe bath, a mixture of 10 ml (0.4M) cadmium acetate, 5 ml triethanolamine, 10 ml (25%) ammonia, 15 ml (0.4M) sodium selenosulphate solution was prepared in a beaker. Similarly, for second bath of 0.5M CdSe, a mixture of 10 ml (0.5M) cadmium acetate, 5 ml triethanolamine, 10 ml (25%) ammonia, 15 ml (0.5M) sodium selenosulphate solution was prepared in a beaker. For Mg doping (0.5M) magnesium chloride solution was added in the second bath. Triethanolamine complexes of Cd^{2+} and Mg^{2+} react with sodium selenosulphate in an aqueous alkaline medium. pH of the solution was adjusted using 25% Ammonia solution. Complexing agent triethanolamine increases the film adherence. In this technique, the deposition is based on the principle of precipitation followed by condensation.

The optimum preparative parameters, such as deposition time and temperature, concentration of species, speed of magnetic stirring, reflux time in condenser for the preparation of selenium precursor, pH of bath etc. were found to influence quality and thickness of the films significantly. At high temperature and for less duration, deposition was found to be of poor quality hence was not continued. Attempts were made to optimize the parameters to obtain good quality films and are reported in [4]. These optimum values were observed as time 24 h, room temperature and pH 11 ± 0.3 respectively. After depositions, the samples were rinsed in triple distilled water and dried naturally at room temperature to avoid cracks in the samples. Different doping concentrations of Mg (Mg/Cd = 0, 1, 2, 3, 4 and 5 at.%) were checked for optimum result.

2.2 Characterization techniques

The optical absorption and transmission spectra of the films were obtained by double beam UV–VIS–NIR Spectrophotometer Spectra scan software 6.51 (Chemito, SPECTRASCAN-UV-2600). The photoluminescence spectra of the films were taken in the range 400–700 nm by using a constant deviation spectrometer. The PL excitation source was a UV source with filters of wavelength 235, 245, 260, 275 and 320 nm. For detection of emitted light, an RCA 931A photomultiplier tube, operated by a highly regulated power supply (EHT-11, Scientific Instruments, Roorkee, India) was used. The integrated light output in the form of current was recorded by digital Pico-ammeter (DPM-121, Scientific Instruments, Roorkee). SES-CAMM computer aided measurement module for Two Probe Experiment, TPX-1.1 (Scientific Instruments, Roorkee) was used to study the variation of electrical resistivity with temperature. An

X-ray diffractometer (D8 Advance) with CuKα irradiation ($\lambda = 1.54060$ Å) was used to identify the crystal structure of the films. The X-ray tube (CuKα source) was operated at 40 kV and 100 mA. The XRD were recorded between angle 2θ ranges from 20° to 65° at a scanning step of 0.02°. The two and three dimensional images of surface of the samples were obtained by atomic force microscopy (AFM) with a Nanoscoped E model contact mode instrument.

3 Results and discussion

Color of the film changes from dark brown / black (deposition at high temperature and less duration) to dark orange, uniform, well adherent and smooth when prepared by above method. Thickness of the films were measured by weight difference method [16] using highly sensitive Shimadzu micro balance (range up to 0.1 mg) and found 215 nm for undoped CdSe and 398 nm for 5% Mg doped sample. Thickness observed in microstructure, recorded with atomic force microscope (AFM) was almost in good agreement.

3.1 Optical study

The optical absorption spectra of Mg doped 0.4 and 0.5 M CdSe thin films are shown in Fig. 1 These spectra were recorded using double beam spectrophotometer in the wavelength range 400–700 nm at room temperature in air. To confirm that the absorption and transmission spectra displayed are as a result of the films deposited on the glass slides, a blank glass slide is placed in one of the beam direction, during scanning process.

It is observed that good homogeneity in the shape and size of the grains and lower defects density near the band edge of the prepared thin film is indicated by a steep optical absorption feature.

After comparison, the size quantization effects of nanoparticles of 0.5 M CdSe and CdSe:Mg (5%) were studied for maximum steep rise in absorption. The study shows the characteristic feature of II–VI compound, i.e. presence of absorption edge in exponential shape [5]. Absorption is found lower at higher wavelengths side whereas it increases steeply for lower wavelengths. The shapes of both the spectra are relatively similar but a difference in absorbance and extinction coefficient was observed in Fig. 2. The extinction coefficient of as-deposited and doped CdSe thin films is found in the order 10^6 (large value is due to strong quantum confinement) and deceased with wavelength, as observed in [19]. It is also varied with percentage of doping and found to decrease which revealed improvement in crystallinity and decrease in surface roughness. The absorption coefficient (α), nature of transition involved and optical band gap (E_g) were calculated utilizing the above spectra.

The absorption data was analyzed using classical Tauc relation [20]. The variation of $(\alpha h\nu)^2$ versus $h\nu$ is linear as shown in Fig. 3, which indicates that the mode of transition in these films is of direct nature. The band-gap energy is observed from 2.62 to 2.37 eV as shown in Fig. 3. The value is quite high when compared with reported values (1.86–1.84, 1.99 eV) in the literature [3, 5, 15]. The variation in band-gap energy may be due to variation in grain structure and size of the CdSe:Mg crystallite.

Calculated band gap values (E_g) are higher than the optical band gap $\left(E_{g(bulk)}\right)$ of bulk CdSe which is around
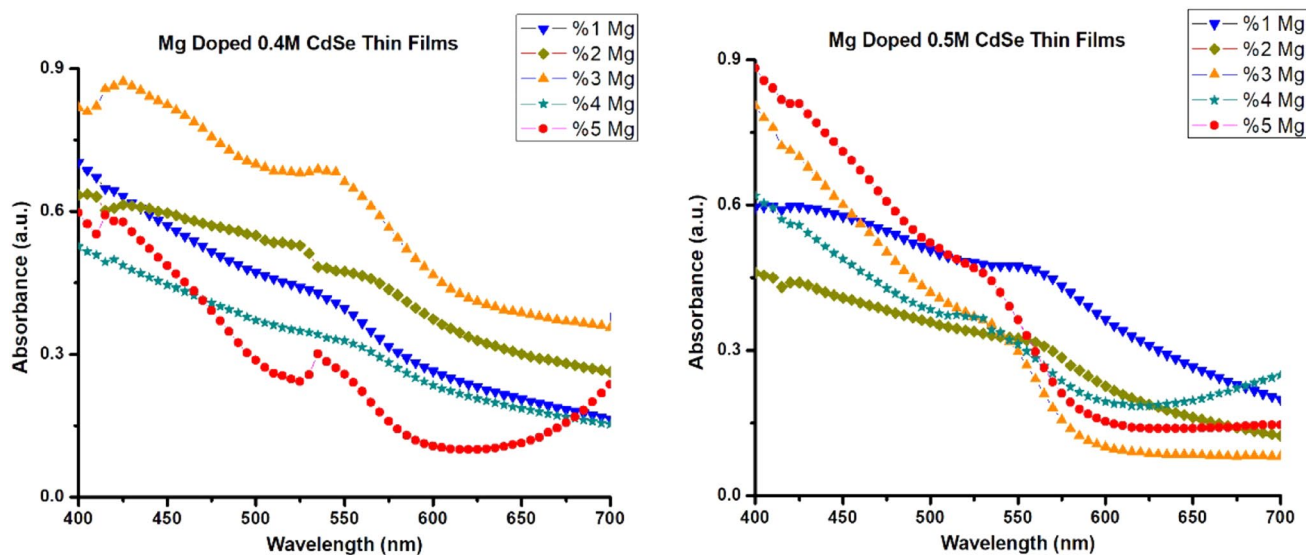
Fig. 1 Absorption spectrum of CdSe thin films with different concentrations of Mg

Fig. 2 Absorbance and extinction coefficient of 0.5 M undoped and doped CdSe thin film
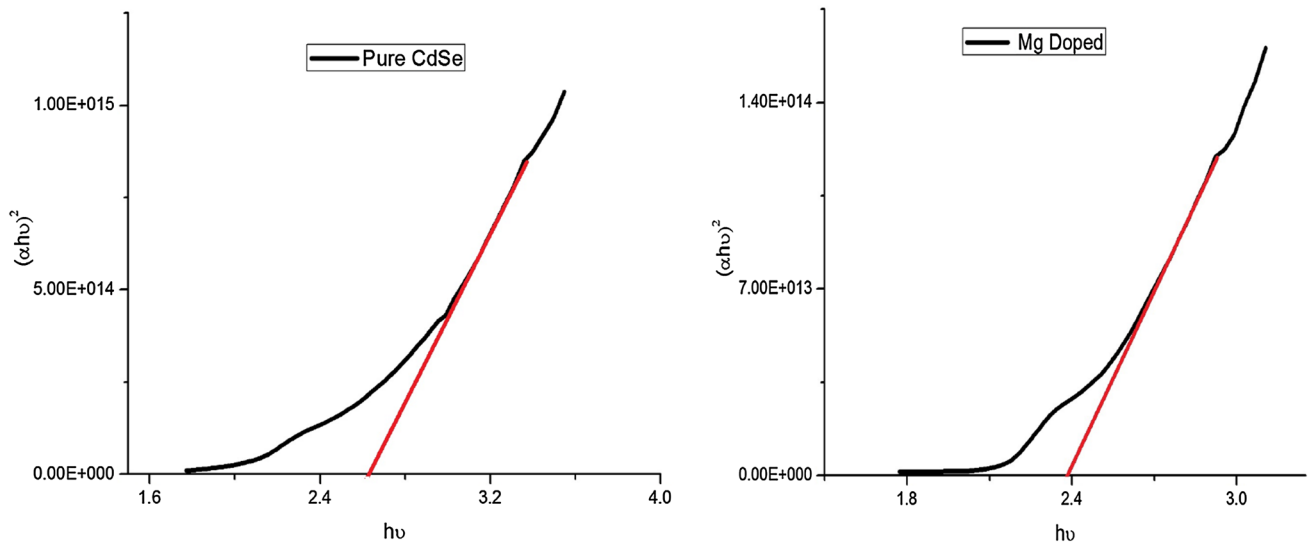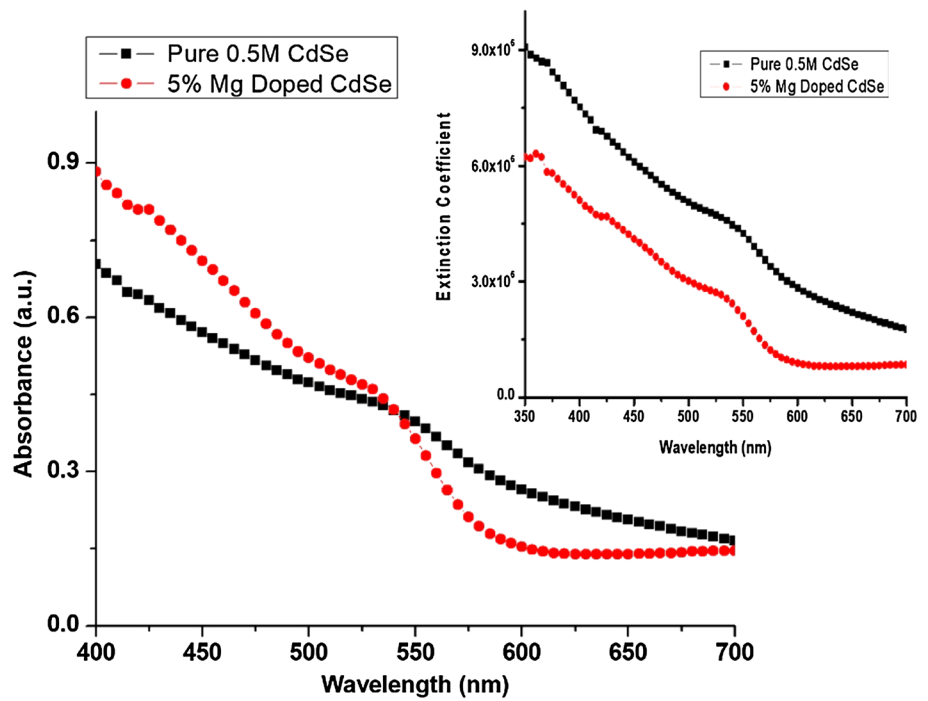
Fig. 3 Determination of band gap in 0.5M undoped and 5% Mg doped CdSe thin films

1.74 eV at room temperature [13], showing blue shift. For accuracy, the particle size was calculated using effective mass approximation,

$$E_g = E_{g(bulk)} + \frac{2\hbar^2\pi^2}{\mu D^2} \tag{1}$$

where D is the diameter of crystallites and μ is the effective mass of electron–hole pair. The average size of nanocrystallites was calculated and listed in Table 1.

Table 1 Size of Crystallites calculated from UV–Vis Data

Films	Band gap E_g (eV)	Band gap shift (eV)	D (nm)	D/D_B
Pure CdSe	2.62	0.88	3.306	0.295
CdSe:Mg	2.37	0.63	3.907	0.349

Bohr exciton diameter (D_B) of CdSe is (11.2 nm). From Table 1, it is clear that the nanocrystallite sizes (D) of the films are much smaller than D_B. Under this condition

localization of electrons and holes takes place in confined volume of the semiconductor [5]. Hence the prepared film shows a single particle confinement behavior in which holes and electrons are independently confined. It confirms the strong quantum confinement effect. Optical and electrical properties of nanocrystals are also based on the knowledge of refractive index (n) and dielectric constant (ε) of semiconducting films to construct solar cell and other optoelectronic devices. The refractive index of the films was calculated using Moss relation [21] which is directly linked to the energy band gap (E_g),

$$E_g n^4 = k \qquad (2)$$

where k is a constant having a value of 108 eV. The high frequency dielectric constant(ε_∞) and static dielectric constant $\left(\varepsilon_0\right)$were calculated using the given relations [21].

$$\varepsilon_\infty = n^2 \qquad (3)$$

$$\varepsilon_0 = -33.26876 + 78.61805 E_g - 45.70795 E_g^2 + 8.32449 E_g^3 \qquad (4)$$

For both films the calculated n, ε_∞ and ε_0 are listed in Table 2. The results are well supported by earlier reported work [19].

3.2 Photoluminescence (PL) study

Quality of semiconductor material is characterized by photoluminescence (PL) studies. PL emission intensity of a phosphor depends upon the concentration of luminescence centers, absorbing efficiency at the excitation wavelength and the quantum yield. It furnishes information about band edge emission and deeper defect related emissions. The near band edge emission of zinc blend (ZB) CdSe is located at about 1.67 eV, while that of wurtzite (W) CdSe is at 1.74 eV at room temperature [3, 5]. Figure 4 shows PL spectrum of as-deposited nc-CdSe thin film at an excitation wavelength of 235 nm. The spectrum shows one strong emission peak centered at 530 nm (2.33 eV) correspond to radiative recombination involving shallow levels in the band gap due to native impurities. The photoluminescence band should show red shifts with increasing particle size after doping.
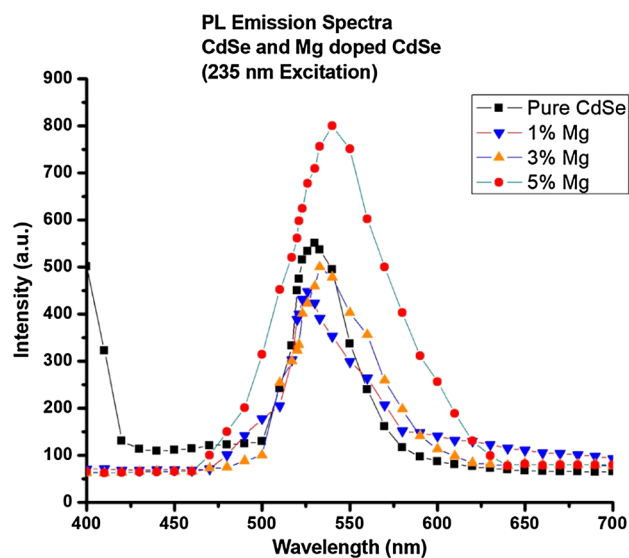
Fig. 4 PL emission peaks at 530 nm (undoped CdSe), 526 nm (doped with 1% Mg), 533 nm (with 3% Mg), 540 nm (with 5% Mg)

The emission from (1–5%) Mg doped samples positioned at 526–540 nm corresponds to 2.35–2.29 eV. Maximum PL emission observed for 5% Mg doped 0.5 M CdSe corresponds to excitonic band to band (e–h) recombination (direct transition). The observed emission transition at 540 nm may be electric dipole allowed and the emitting level has a very short lifetime. This explains very strong luminescence intensity [8, 9]. The obtained value is close to band gap of polycrystalline CdSe: Mg thin film (i.e. 2.37 eV) confirming the ZB phase of sample [10]. We have observed well enhanced PL intensity contrary to annealing effect though the same pattern of change in band gap is observed by Shyju et al. [22]. Formation of different intrinsic defects after incorporation of Mg^{2+} in CdSe lattices may also be the reason of enhanced visible emission [11]. Besides, we observed no other emission peaks confirming the excellent quality of CdSe films.

PL is very sensitive to the quality of crystal structure and to the presence of defects. For adding 1% Mg, these emission peaks are shifting towards the lower wavelength side (526 nm) due to the band-gap increase as compared to the undoped CdSe. There after the band gap decreases with increasing doping concentration. It is known that the PL emission is caused by the recombination of excited electrons and holes, and the lower PL intensity may indicate the lower recombination rate of electrons and holes under light irradiation. It is reasonable that there are some defects in the CdSe:Mg nanostructures at the surface and subsurface due to their fast reaction formation process and large surface to volume ratio. The PL intensity is highest as prepared sample (doped with 5% Mg) indicating the highest recombination of electrons and holes. By simply

Table 2 Values of band gap(E_g), refractive index(n), high frequency dielectric constant (ε_∞) and static dielectric constant (ε_0) for Nanocrystalline Pure CdSe and CdSe:Mg Thin Films calculated from UV–Vis data

Films	Band gap E_g (eV)	n	ε_∞	ε_0
Pure CdSe	2.62	2.53	6.40	8.67
CdSe:Mg	2.37	2.59	6.71	7.14

varying the size of these as-deposited and doped nanocrystalline thin films may find applications in best emitters those are highly efficient, highly pure in emission and continuously tunable [22].

3.3 Electrical properties

The two-point dc probe method of dark electrical resistivity measurement was used to study the variation of electrical resistivity with temperature. The measurements were taken in the varying temperature range of 323–403 K. Fig. 5 shows a plot of log (ρ) versus inverse absolute temperature. This confirms the semiconducting nature of the films because resistivity decreases by increasing the temperature. The resistivity of the pure CdSe and CdSe: Mg thin films are in the range of 10^7–10^5 Ωcm. The high resistivity of the pure CdSe thin films may be due to the presence of various disorders inside the film. The straight line shows that pure CdSe thin film has only one type of conduction while Mg doped CdSe thin films have two types of conduction mechanisms which contribute to the conductivity. Low temperature conductivity can be considered as the extrinsic conduction due to the presence of impurity atoms. High temperature conductivity is due to the intrinsic conduction. Figure 5 shows that due to doping of Mg, only small decrease in resistivity was observed specially at lower temperature which can be attributed to the change in structural parameters, increase in crystallite size and film crystallinity. The plot shows that for low temperature the resistivity of doped films is almost constant and it appears to be thermally stimulated in the high temperature range.
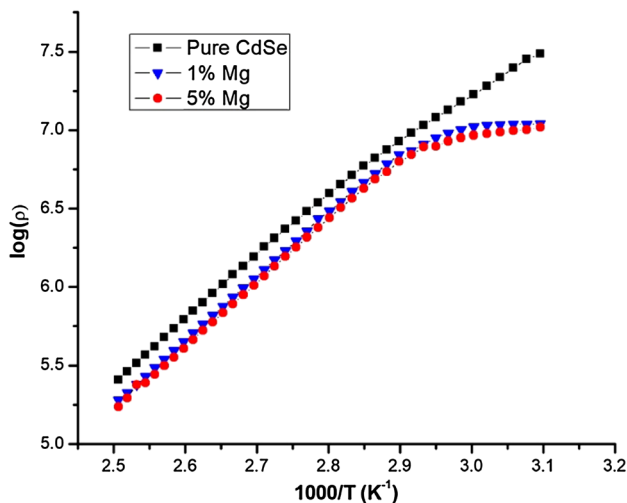
The activation energy E_a represents the location of trap levels below the conduction band and it was calculated by the relation,

$$\rho = \rho_0 \exp(E_a/KT) \tag{5}$$

where ρ is the electrical resistivity, ρ_0 is the pre-exponential factor, K is the Boltzmann constant, T is the absolute temperature.

The activation energy of our samples was found to be in the range of 0.19–0.21 eV for lower temperature region and 0.80–0.84 eV for higher temperature region that matches well with earlier results [3, 16, 19].

3.4 X-ray diffraction study

Dependence of synthesis conditions such as deposition temperature and precursor concentration affects the crystal structure of cadmium chalcogenides. Normally duality is observed either with cubic (ZB-zinc blend type) or W-wurtzite (hexagonal type) structure [2, 15]. The XRD profiles of chemically deposited undoped and 5% Mg doped nanocrystalline CdSe thin films are shown in Fig. 6. The strong orientation is along (1 1 1) plane and also some other reflections (2 2 0) and (3 1 1) have been observed in CdSe polycrystalline thin films [15, 19]. In CdSe:Mg film along with CdSe peaks, the presence of very weak peak around 32° in Fig. 6 may correspond to MgSe peak (2 0 0)$_C$ [16]. No additional peaks of other compounds are present. The broad and low intense peaks may be due to the formation of small size nanoparticles in CdSe thin film. It has been observed that both the films have same crystal structure but the intensities and full width at half maximum (FWHM) values of these peaks change with doping. Diffraction peak intensities increased with increasing film thickness for CdSe:Mg thin film. These changes can be considered due to the improvement of crystallinity of the films by film thickness.

Fig. 5 Plot of log (resistivity) versus inverse of absolute temperature for the thin films
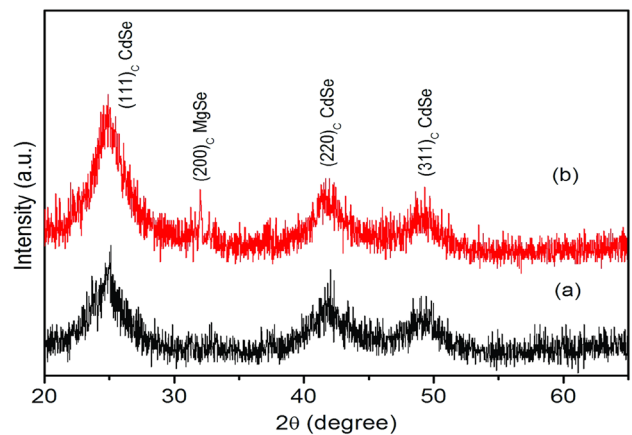
Fig. 6 XRD pattern of (*a*) 0.5 M CdSe and (*b*) 5% Mg doped CdSe

The XRD data are indexed with the help of JCPDS files (File No: 19-0191, 08-459 and 18-0777). A matching of the observed and the standard interplanar spacing d (A^0) values confirms that cadmium selenide exists in the zinc blende type cubic structure. The XRD pattern shows the highest intensity reflection peak at d=3.5333 Å (111). The lattice constant (a) and inter planar spacing (d) of different films show a good agreement with the reported values [1–3, 15, 16, 19] and have been listed in Table 3.

Nelson Riley plot as shown in Fig. 7 was used to determine modified value of lattice parameter for different planes. It is a plot of lattice parameter a (Å) versus error function $F(\theta)$ and was found to be straight line. Error function is calculated using equation.

$$F(\theta) = \cos\theta \left[\frac{\cos\theta}{\sin\theta} + \frac{\cos\theta}{\theta} \right] \tag{6}$$

Table 3 XRD data of Nanocrystalline Pure CdSe and CdSe:Mg Thin Films

Films	(hkl)	Intensity	Interplanar spacing d (A^0)	Lattice constant a (A^0)
CdSe 19–0191 (JCPDS)	$(1\,1\,1)_C$	100	3.5127	6.0841
	$(2\,2\,0)_C$	55	2.1511	
	$(3\,1\,1)_C$	25	1.8344	
Pure CdSe	$(1\,1\,1)_C$	100	3.5333	6.1198
	$(2\,2\,0)_C$	52	2.1588	6.1060
	$(3\,1\,1)_C$	44	1.8429	6.1122
CdSe:Mg	$(1\,1\,1)_C$	100	3.5273	6.1094
	$(2\,2\,0)_C$	42	2.1585	6.1051
	$(3\,1\,1)_C$	33	1.8387	6.0982

Intersection of this plot at Y-axis gives a value of lattice parameter, which is usually free from systematic errors [23]. The expected values of lattice constant for the films were $a = 6.110$ Å which were close to the reported values $a = 6.0841$ Å.

According to the Debye Scherrer's equation, the average size of the nanocrystals can be determined as: $D = k\lambda/\beta\cos\theta$ where D is the average crystallite size of the nanocrystals, λ is the wavelength of the X-ray radiation used, β is the full-width of half-maximum intensity of the peak, θ is the angle at which the diffraction peak occurs, and k is a constant that has a value of 0.94 for CdSe [24]. From the preferred (1 1 1) diffraction peaks, the estimated crystallite size of the CdSe nanocrystals prepared with 5% Mg doping is increased from 2.967 to 3.227 nm. Similar results are found in CdSe films with annealing temperature [3, 5, 20, 25].

Crystallite size and strain can also be obtained using Williamson–Hall (W–H) plot by knowing the FWHM of the diffraction peaks. Considering the peak width as a function of 2θ, both size-induced and strain-induced broadening is simplified by W–H method [24]. The strain developed due to crystal imperfection was calculated using the formula [20]

$$\gamma = \beta \cot\theta/4. \tag{7}$$

The calculated strains of pure CdSe and CdSe:Mg thin films are given in Table 4. When Mg content is increased, the grain boundaries decreased and strain is reduced considerably due to the enlarged crystallite size. Thus, strain relaxation favors grain growth and thereby better crystallinity up to optimum level of doping. FWHM (β) can be simply the sum of broadening from crystallite size and strain.

$$\frac{\beta\cos\theta}{\lambda} = \frac{k}{D} + \frac{4\gamma\sin\theta}{\lambda}. \tag{8}$$

For multiple ordered diffraction pattern a plot is drawn with $(\sin\theta)/\lambda$ along the x-axis and $(\beta\cos\theta)/\lambda$ along the
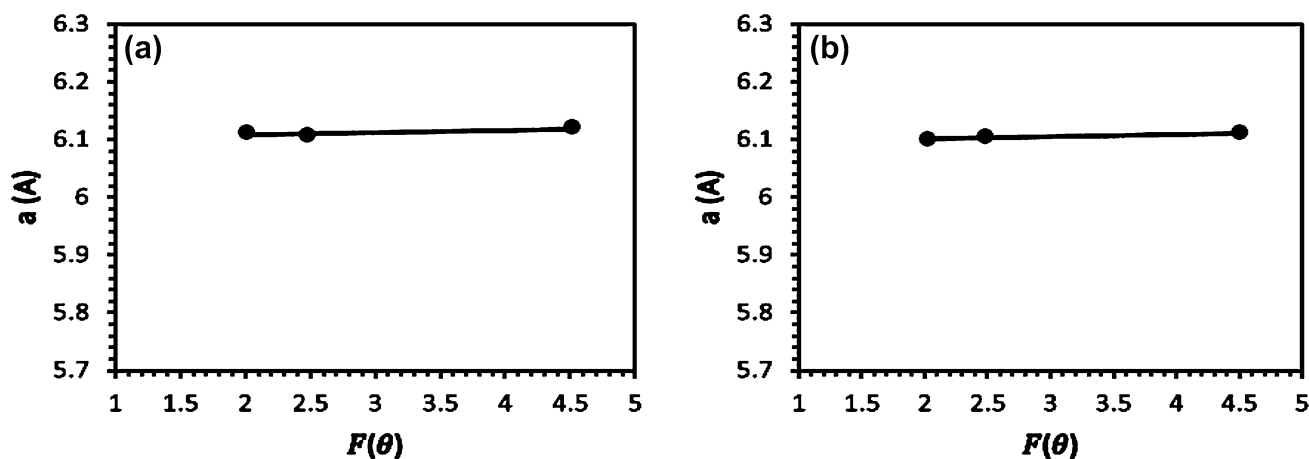
Fig. 7 Nelson–Riley plots for (**a**) pure CdSe thin film (**b**) CdSe:Mg thin film

Table 4 Values of crystallite size (D), strain (γ), dislocation density (δ) for nanocrystalline pure CdSe and CdSe:Mg thin films

Films	Crystallite size (Scherrer's formula) D (nm)	Crystallite size (W-H plot) D (nm)	Strain γ ($\text{lin}^{-2}\,\text{m}^{-4}$)	Dislocation density δ ($\times 10^{17}$ lin/m^2)
Pure CdSe	2.967	2.941	0.052	1.135
CdSe:Mg	3.227	3.125	0.045	0.960

y-axis. Average crystallite size (D) was estimated from the reciprocal of intercept on the y-axis and strain (γ) from the slope of the fit. Figure 8 shows the plot of $\beta \cos \theta / \lambda$ versus $\sin \theta / \lambda$ for CdSe & CdSe:Mg films which gives straight line. The average crystallite size shows close agreement with the value obtained from Debye Scherrer's formula.

The dislocation density δ has been calculated using the Williamson and Small man's relation [26].

$$\delta = {}^1\!/_{D^2} \tag{9}$$

where D is the crystallite size. The estimated dislocation densities for nanocrystalline CdSe and CdSe:Mg thin films have been listed in Table 4. The value of dislocation density is less for the doped films, which may be due to the growth in crystallite size. For doping, the changes in microstructural properties and increase in crystallinity may be the reason for the reduction in the amount of lattice deficiencies leading to preferred orientations.

On comparing the average crystallite size with literature value of the Bohr's radius in bulk CdSe, it can be seen that the calculated crystallite size is less than Bohr's radius (6.1 nm) which shows that all deposited films are strongly quantized. It is found that calculated lattice parameter shows small increase in value when compared with the reported JCPDS value which might be due to the small grain in films and it is due to high surface to volume ratio. Dislocation density and strain decrease with Mg doping thereby suggesting that films are becoming more compact and perfect in nature.

3.5 AFM studies

AFM is a promising technique to study the surface topography of samples because it provides valuable information regarding the growth mechanism, shape and size of grains and rms roughness of the surface of the sample. Figure 9 shows the typical 2D and 3D view of AFM images of 5×5 μm^2 area of CdSe and CdSe:Mg thin films. It is observed that the film surface is uniform, homogenous and well covers the substrate. The deposited CdSe film shows growth of tiny hilly structured grains with some gaps. However, the addition of Mg in bath clearly shows that the grains are now more spherical and more compact as reported [15, 19]. This type of morphology can be used to improve the quality of many optoelectronic devices. The surface roughness has been measured by using the reported software [27]. The average grain size of the film was measured 52.3 nm using AFM images, which is higher than that determined by XRD. This finding indicates that many nanocrystallites oriented in the same plane coalesced to form the above grain size. The surface roughness of the films is measured to be 32.65 and 25.21 nm for CdSe and CdSe:Mg films respectively. Thickness of the films was measured 183.88 and 201.53 nm for CdSe and CdSe:Mg films respectively. Film thickness can be considered as the perpendicular distance from top grains surface to top substrate surface. It is clear that due to Mg doping in CdSe, the grain size and smoothness of the film improved.
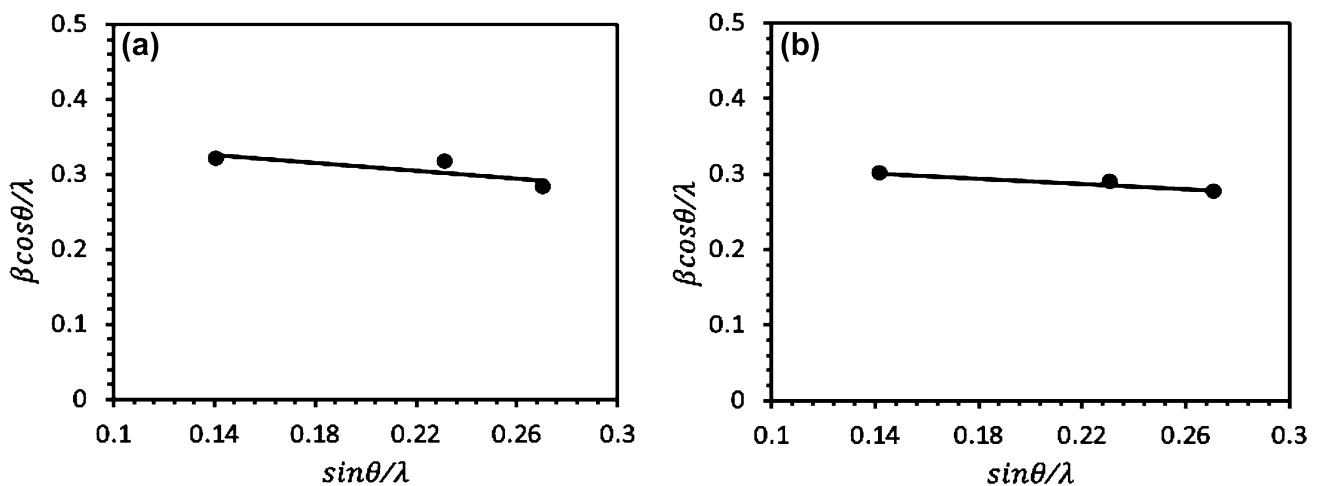
Fig. 8 W–H plots for (**a**) pure CdSe thin film (**b**) CdSe: Mg thin film
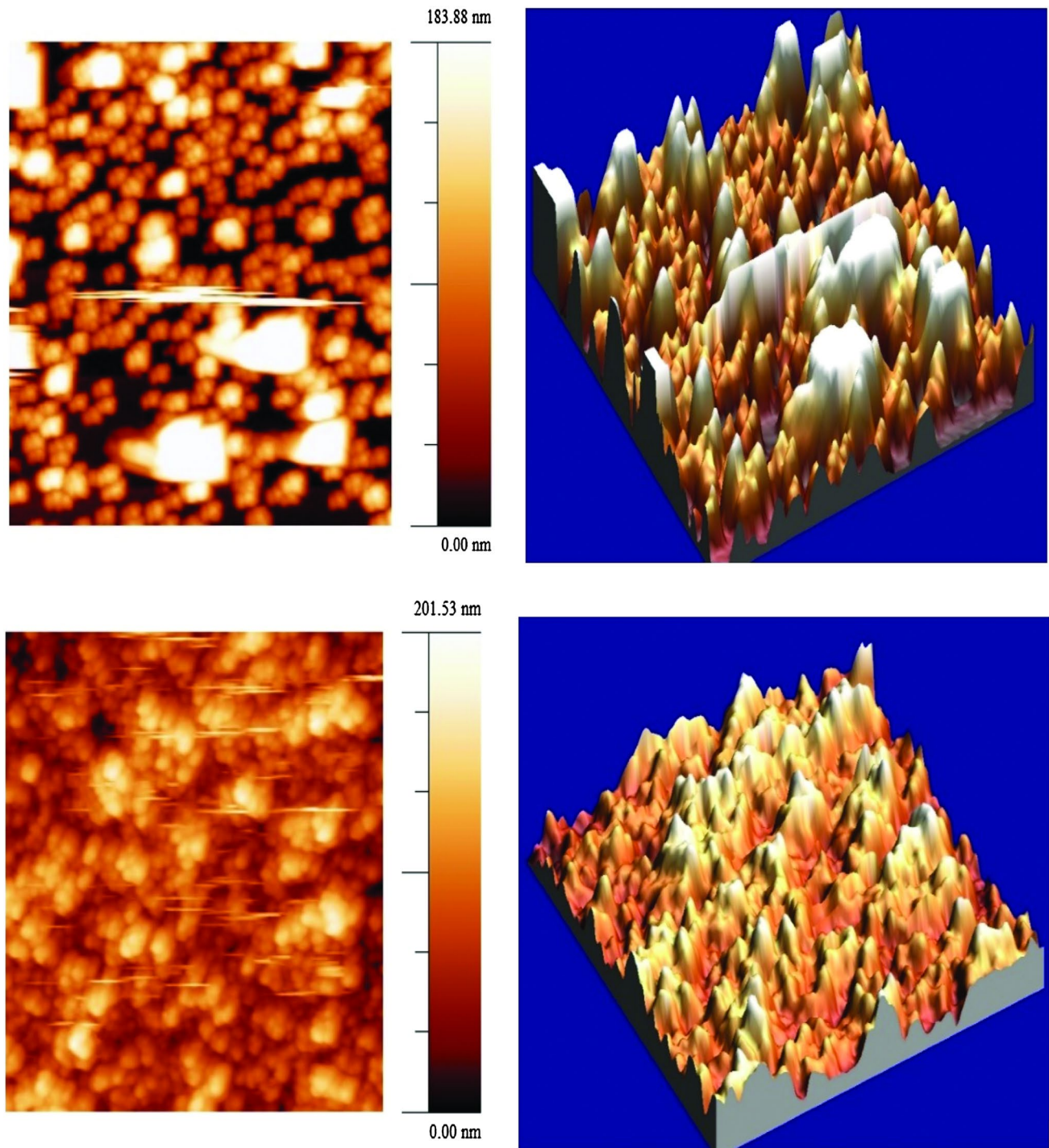
Fig. 9 AFM images (2-dimensional and 3-dimensional) of pure CdSe and CdSe:Mg thin film

3.6 Compositional study

Little amount of the sample was dissolved in small quantity of concentrated nitric acid. It has been reported that below pH 7 the selenium is precipitated as free metal and nitrates of cadmium persist in the solution. Precipitate was filtered using a Gooch crucible, then weighed using microbalance gives selenium percentage in the sample. The compositional analysis of the CdSe film using this method gave 52.15% cadmium and 47.85% selenium. CdSe:Mg film gave 51.8% cadmium and magnesium and 48.2% selenium, which show samples, are selenium
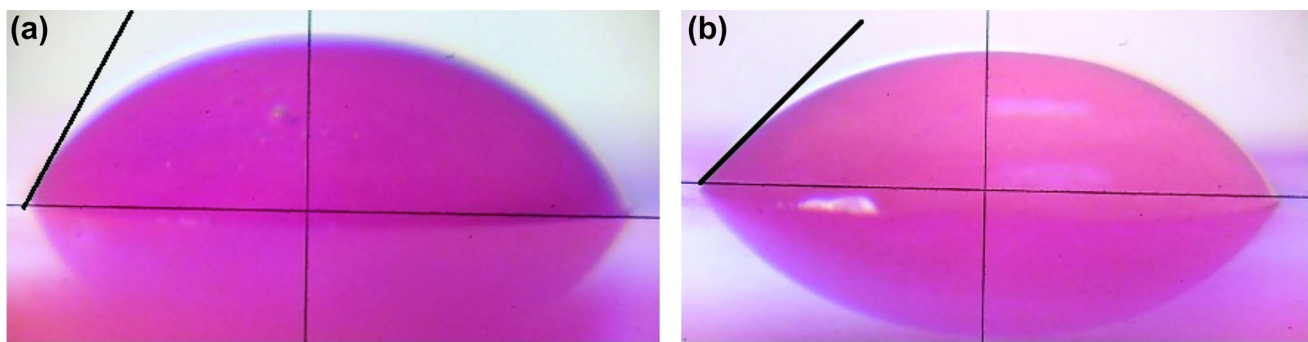
Fig. 10 Surface water contact angle images on (**a**) pure CdSe surface, (**b**) CdSe:Mg surface

deficient and cadmium rich. This result matches with the earlier reports [3, 5].

3.7 Surface wettability test

Many applications require modification in the solid surfaces wettability. Surface wettability is characterized by contact angle; it involves the interaction between a solid and a liquid in contact. It relates to the surface energies of the system [28]. Water contact angle was measured using travelling microscope with least count 0.001 cm [29]. Figure 10 shows this value for CdSe and CdSe:Mg films and is about 62° and 47° respectively. It confirms hydrophilic behavior as for both the films water contact angle is less than 90°. CdSe:Mg film has low contact angle. Increase in crystallite size and change in microstructural properties may be the reason for changes in surface properties, due to which high wetting behavior is obtained here. Low contact angle means better interfacial contact between electrode and electrolyte hence these films are suitable for making photo electrochemical cell.

4 Conclusion

Semiconducting and hydrophilic nanocrystalline thin films of magnesium doped (Mg/Cd = 0, 1, 2, 3, 4 and 5 at. %) cadmium selenide have been prepared using the less expensive chemical bath deposition technique. The presence of self-grown CdSe:Mg nanoparticles were confirmed from optical absorption study. The films showed strong red-shift in optical band gap with increase in doping concentration, indicating the charge confinement effect in nanocrystallites of the film. The extinction coefficient was found in the order 10^6 and which decreased slightly with doping. The refractive index was also calculated and found in the range 2.53–2.59. It was found that with 5% doping of Mg in deposition bath, optical band-gap and electrical resistivity decreases drastically. The room temperature electrical resistivity of CdSe thin films is of the order of $10^7\ \Omega$ cm. Photoluminescence

studies revealed that the deposited films have distinct emission peaks in the range of 526–540 nm under 235 nm illuminations depending on the concentration. Doping CdSe with 5% Mg shows increased photoluminescence intensity, which results from strong quantum confinement. From the photoluminescence analysis, it is inferred that the deposited samples have direct band transition and also red shift is observed. This shows CdSe is a potential candidate for solar cell fabrication.

The XRD study indicates polycrystalline nature in cubic phases with highest reflection along (111) plane. This is because of the doping with Mg at concentrations of ∼ 5% the increase of grain size and removal of defects, which are present in the film. Crystallinity improvement followed by decrease in surface roughness from 32.65 to 25.21 nm and reduction in water contact angle from 62° to 47° (±0.20)° due to doping showed increase in crystallite size from 2.941 to 3.125 nm. The dislocation density and strain varies in the range $(1.135–0.960) \times 10^{17}\ \mathrm{lin^{-1}m^2}$ and (0.052–0.045) $\mathrm{lin^{-2}m^{-4}}$ respectively. Our results are in good agreement with the standard data and available literature. Briefly, the structural and opto-electronic properties of CdSe films can be tuned with alkaline earth metal ions for their novel device applications. It can be concluded that the deposited films maybe used in field emission displays due to its high efficiency emission in the presence of Mg.

References

1. S. Mahato, A.K. Nanda Shakti, Kar, Mater. Sci. Semicond. Process. **39**, 742 (2015)

2. S.K. Sharma, A.S. Al-Kabbi, G.S.S. Saini, S.K. Tripathi, J. Alloys Compd. **564**, 42 (2013)
3. M.L. Gaur, P.P. Hankare, K. M.Garadkar, S.D. Delekar, V.M. Bhuse, J. Mater. Sci. **25**, 190 (2014)
4. R. Das, K. Prashant, Sahu, J. Optoelectron. Adv. Mater. **12**(6), 1406 (2010)
5. P.A. Chate, D.J. Sathe, P.P. Hankare, S.D. Lakaded, V.D. Bhabad, J. Alloys Compd. **552**, 40 (2013)
6. S. Bhanoth, A.S. Kshirsagar, P.K. Khanna, A. Tyagi, A.K. Verma, Adv. Nanoparticles **5**, 1 (2016)
7. J.-H. Ahn, R.S. Mane, V.V. Todkar, S.-H. Han, Int. J. Electrochem. Sci. **2**, 517 (2007)
8. S. Chawla, N. Kumar, H. Chander, J. Lumin. **129**, 114 (2009)
9. S. Chawla, K. Jayanthi, H. Chander, Phys. stat. sol. a **205**(2), 271 (2008)
10. H. Joy Prabu, I. Johnson, Int. J. Eng. Res. Appl. **5**(8), 99 (2015)
11. D.A. Reddy, D.H. Kim, S.J. Rhee, B.W. Lee, C. Liu, Nanoscale Res. Lett. **9**(1), 20 (2014)
12. J. Zhang, F. Jiang, Phys. Lett. A **373**, 3888 (2009)
13. Y.P. Gnatenkon, P.M. Bukivskij, I.O. Faryna, A.S. Opanasyuk, M.M. Ivashchenko, J. Lumin. **146**, 174 (2014)
14. W.-C. Kwak, T.G. Kim, W.-S. Chae, Y.-M. Sung, Nanotechnology **18**(20), 205702 (2007)
15. Y. Zhao, Z. Yan, J. Liu, A. Wei, Mater. Sci. Semicond. Process. **16**, 1592 (2013)
16. A.U. Ubale, Y.S. Sakhare, Vacuum **99**, 124 (2014)
17. A.U. Ubale, Y.S. Sakhare, S.G. Ibrahim, M.R. Belkhedkar, Solid State Sci. **2**, 1 (2014)
18. K. Sarmah, R. Sarma, H.L. Das, Chalcogenide Lett. **5**(8), 153 (2008)
19. A. Purohit, S. Chander, S.P. Nehra, M.S. Dhaka, Phys. E **69**, 342 (2015)
20. R. Kumar, R. Das, M. Gupta, V. Ganesan, Super Lattice Microstruct. **75**, 601 (2014)
21. L. Hanna Chi, N. Bouarissa, Phys. B **404**, 3650 (2009)
22. T.S. Shyju, S. Anandhi, R. Indirajith, R. Gopalakrishnan, J. Alloys Compd. **506**, 892 (2010)
23. C. Whiston, *X-Ray Methods*. (Wiley, New York, 1991)
24. C. Suryanarayana, M.G. Nortan, *X-ray Diffraction: A Practical Approach* (Springer, New York, 1998)
25. M.N. Sumbit Chaliha, P.C. Borah, A. Sarmah, Rahman, J. Optoelectron. Adv. Mater. **10**(2), 427 (2008)
26. G.K. Williamson, R.E. Smallman, Philos. Phenomenol. **1**, 34 (1956)
27. I. Horcas, R. Fernandez, J.M. Gómez-Rodríguez, J. Colchero, J. Gómez-Herrero, A.M. Baro, Rev. Sci. Instrum. **78**, 013705 (2007)
28. A.V. Shaikh, R.S. Mane, O.S. Joo, B.N. Pawar, J.K. Lee, S.H. Han, J. Phys. Chem. Solids **72**, 1120 (2011)
29. A. Sanjay, C.H. Gawali, Bhosle, Mater. Chem. Phys. **129**, 751 (2011)